

Nature

Single-molecule spectral fluctuations at room temperature

Author(s): Lu, H. Peter; Xie, X. Sunney

ISSN: 0028-0836

Issue: Volume 385(6612), 9 January 1997, pp 143-146

Accession: 00006056-199701090-00021

Publication Type: [Letter to Nature]

[Email Jumpstart](#)

Publisher: © 1997 Macmillian Magazines Ltd

[Find Citing Articles](#)

Pacific Northwest National Laboratory, Environmental

[« Table of Contents](#)Institution(s): [Molecular Sciences Laboratory, PO Box 999, Richland, Washington 99352, USA.](#)[About this Journal »](#)

Table of Contents:

[« Entropy difference between the face-centred cubic and hexagonal close-packed crystal structures.](#)[» Silurian hydrothermal-vent community from the southern Urals, Russia.](#)

Links

[Abstract](#)[Complete Reference](#)[ExternalResolverBasic](#)

Outline

- [Abstract](#)
- [REFERENCES](#)

Graphics

- [Figure 1](#)
- [Figure 2](#)
- [Equation 1](#)
- [Equation 3](#)
- [Figure 3](#)
- [Figure 4](#)
- [Equation 2](#)
- [Figure 5](#)

Abstract 

Recent advances in near-field [1] and far-field [2,3] fluorescence microscopy have made it possible to image single molecules and measure their emission [3,4] and excitation [5] spectra and fluorescence lifetimes [3,6-8] at room temperature. These studies have revealed spectral shifts [4] and intensity fluctuations [6,7], the origins of which are not clear. Here we show that spontaneous fluctuations in the spectra of immobilized single dye molecules occur on two different timescales: hundreds of milliseconds and tens of seconds, indicating that these fluctuations have two distinct activation energies. In addition, we see photoinduced spectral fluctuations on repeated photoexcitation of single molecules. We suggest that all of these fluctuations can be understood as transitions between metastable minima in the molecular potential-energy surface.

We obtained diffraction-limited fluorescence images of individual sulphorhodamine 101 molecules with a modified inverted fluorescence microscope (Nikon), in a similar fashion to a recent report [3]. The sample was prepared by first spin-coating a quartz surface with a 10 sup -9 M dye solution and then with a 20-nm polymethylmethacrylate film to prevent fast photobleaching. [Figure 1](#) (a) shows the emission spectra of a single molecule sequentially recorded with 170-ms

collection times. The trajectory of the spectral means is shown in [Figure 1](#) (b). The fluctuations of the spectral means are evident, while the spectral widths remain essentially constant. In addition, the total emission intensity (that is, the

integrated area of each spectrum) fluctuates with time [Figure 1\(c\)](#) and is consistent with other observations using near-field microscopy [\[6,7\]](#). The intensity fluctuations were previously attributed to spectral shifts. [\[6\]](#) Indeed, the intensity fluctuations [Figure 1\(c\)](#) essentially correlate with the spectral fluctuations in [Figure 1\(b\)](#): a blue-shifted emission (and absorption) spectrum results in a larger absorption cross-section at the excitation wave-length (532 nm, at the blue edge of the absorption band). The spectra shown in [Figure 1](#) were taken with an excitation rate of $5 \times 10^5 \text{ s}^{-1}$, which is much lower than the saturation rate [\[9\]](#). At saturation, intensity fluctuation arises from a different origin: trapping into the metastable triplet state [\[10,11\]](#).

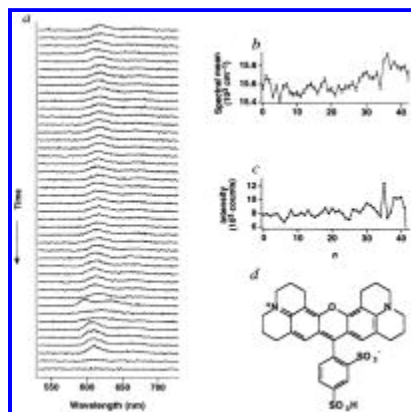


Figure 1. a, Emission spectra of a single sulphorhodamine 101 molecule taken sequentially with 170-ms data collection times before the final photobleaching. Significant spectral shifts are evident. b, Trajectory of the spectral mean (in wavenumbers) of the molecule; n is the index number of the spectra. The fluctuations are clearly beyond the error bars. c, Trajectory of the total emission intensity (integrated area of each spectrum) of the molecule. d, Structure of the molecule. The emission spectra of individual molecules were recorded with a high emission collection efficiency (10%) using a combination of a spectrograph (Acton Research, Acton) and a back-illuminated CCD camera (Princeton Instruments, Trenton) configured for a spectral resolution of 1 nm with no dead time in data collection.

[\[Help with image viewing\]](#)

[\[Email Jumpstart To Image\]](#)

Every molecule that we examined in a large population exhibited similar spectral fluctuations. To evaluate these statistically, we analysed the autocorrelation function $C(t) = \langle v(0)v(t) \rangle - \langle v \rangle^2$ of spectral trajectories, v being the spectral mean in wavenumbers. Each trajectory contained at least several hundred spectra. [Figure 2](#) shows a typical $C(t)$ of a molecule; the trajectory was recorded with an excitation rate of $2.6 \times 10^5 \text{ s}^{-1}$ at 594 nm. The distribution of spectral means ([Figure 2](#) inset) reflects the transition frequencies accessed by the single molecule in the particular environment. Molecules in different environments have distributions that are significantly different in centre positions (620-680 nm) and in widths (full-widths at half-maximum, 4-20 nm).

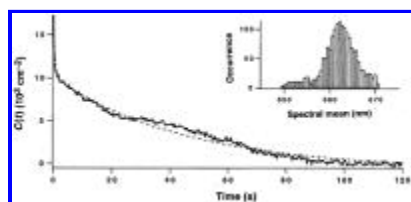


Figure 2. The autocorrelation function, $C(t) = \langle v(0)v(t) \rangle - \langle v \rangle^2$, derived from the trajectory of spectral means of a single sulphorhodamine 101 molecule at an excitation rate of $2.6 \times 10^5 \text{ s}^{-1}$ at 594 nm. The dashed line is a fit to the data using [Equation 3](#) in the text; parameter values are $k_1 = 1.9 \text{ s}^{-1}$, $k_2 = 0.022 \text{ s}^{-1}$, $\sigma_0^2 = 2,000 \text{ cm}^{-2}$ and $\sigma_2^2 = 10,700 \text{ cm}^{-2}$. Inset, the distribution of the spectral means derived from the same trajectory.

[\[Help with image viewing\]](#)

[\[Email Jumpstart To Image\]](#)

$$C(t) = \sigma_0^2 \exp(-k_1 t) + \sigma_1^2 \exp(-k_2 t) \quad \text{for } t > 0$$

Equation 3

[\[Help with image viewing\]](#)

[\[Email Jumpstart To Image\]](#)

The autocorrelation function has a spike at zero time [Figure 2](#), due to uncorrelated measurement noise for spectral means (see [Figure 1\(b\)](#) for error bars) and spectral fluctuations faster than the time resolution. $C(t)$ can be fitted by a double exponential decay with the spike at zero time: [Equation 1](#) [Equation 3](#) The dashed line in [Figure 2](#) is a fit with a spike, $\sigma_0^2 = 2,000 \text{ cm}^2 \text{ sup}^{-2}$; a fast component, $k_1 = 1.9 \text{ s}^{-1}$ and $\sigma_1^2 = 5,000 \text{ cm}^2 \text{ sup}^{-2}$; and a slow component, $k_2 = 0.022 \text{ s}^{-1}$ and $\sigma_2^2 = 10,700 \text{ cm}^2 \text{ sup}^{-2}$.

$$C(0) = \sigma_0^2 + \sigma_1^2 + \sigma_2^2 \quad \text{for } t = 0$$

Equation 1

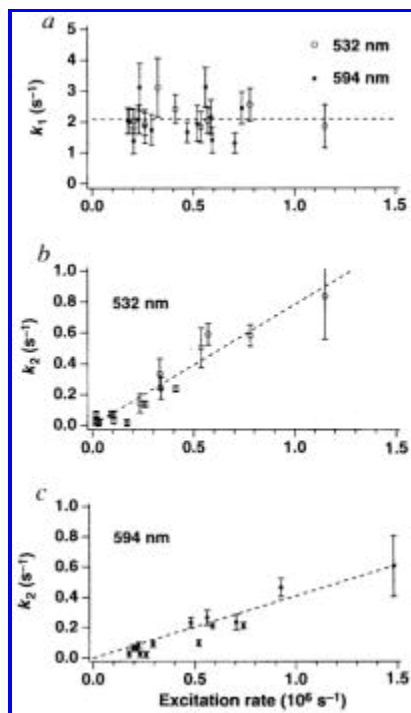
[\[Help with image viewing\]](#)

[\[Email Jumpstart To Image\]](#)

To understand the mechanism of these components of spectral fluctuations, we note that molecules do not exhibit noticeable lateral translation beyond a range of a few nanometres. In addition, no detectable variations in the orientation of the transition dipole were observed in this system [\[6\]](#). Thus we attribute the spectral fluctuations to changes of nuclear coordinates—either the intramolecular coordinates (such as conformations of a side chain) or the intermolecular coordinates (such as hydrogen bonds and collective nuclear coordinates of the interacting environment). The observation that the autocorrelation function of the single molecule has a fast and a slow component implies the existence of at least two quasi-independent distributions of spectral means, with variances of σ_1^2 and σ_2^2 . These two distributions relate to different variations in nuclear coordinates taking place at different rates (k_1 and k_2).

We evaluate the excitation-rate dependence of k_1 and k_2 for many trajectories of many molecules to determine whether the spectral fluctuations are spontaneous or photoinduced. We observed that the fast component (k_1) is independent of excitation rate and excitation wavelength [Figure 3\(a\)](#), and that the slow component (k_2) is excitation-rate-dependent and is different for 532-nm [Figure 3\(b\)](#) and 594-nm excitation wavelengths [Figure 3\(c\)](#). The excitation rate was varied by adjusting the power of linearly polarized excitation light (0.1–2 micro W) and by choosing different molecular orientations. The excitation rates were determined from the integrated area per spectrum by assuming a fluorescence quantum yield close to unity and an emission collection efficiency of 10%. The amplitude ratio of the fast and slow components (σ_1^2/σ_2^2) is essentially independent of the excitation rate, but varies from molecule to molecule.

Figure 3. a, The dependence of K_1 , the fast component of $C(t)$, on the excitation rate. The data points are from different molecules at either 532-nm (open circles) or 594-nm (filled circles) excitation. The independence of K_1 ([approximately] 2.1 s^{-1}) on excitation rate and wavelength indicates that the spectral fluctuation is spontaneous. b, The dependence of K_2 , the slow



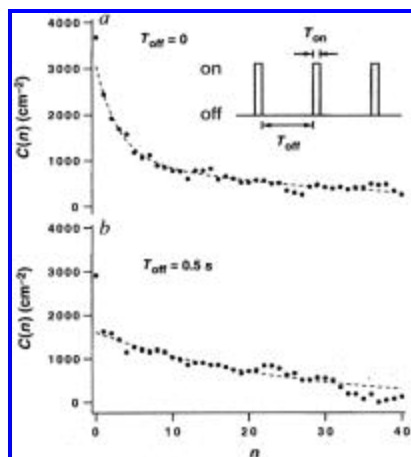
component of $C(t)$, on the excitation rate with 532-nm excitation. The data points are from different molecules. The quasi-linear relationship indicates that the spectral fluctuation is photoinduced. The quantum efficiency for photoinduced spectral change is 7.8×10^{-7} according to the slope c . The dependence of k_2 on the excitation rate with 594-nm excitation. A quasilinear relationship is also observed but with a slower photoinduced fluctuation. The quantum efficiency for photoinduced spectral change is 4.1×10^{-7} . The larger error bars at high excitation rates are associated with the shorter trajectories due to photobleaching.

[\[Help with image viewing\]](#)

[\[Email Jumpstart To Image\]](#)

The observation that the fast component is independent of the excitation rate indicates that the fast fluctuation is spontaneous (known as spectral diffusion) rather than photoinduced. To further confirm this conclusion, we used a shutter to repeatedly block the excitation light for a period of 'dark time', T_{off} , after each spectrum collection time, T_{on} , and obtained the autocorrelation function, $C(n)$ (n being the index number of spectra) (Figure 4 inset). Figure 4(a) shows the $C(n)$ of a molecule with $T_{\text{off}} = 0$; Figure 4(b) shows the $C(n)$ for the same molecule with a $T_{\text{off}} = 0.5$ s at an identical excitation rate during T_{on} . If no spontaneous fluctuations occurred during the dark times, the two curves of $C(n)$ would be identical. We observe, however, that the fast component of $C(n)$ disappeared in Figure 4(b), which provides additional evidence of the spontaneous fluctuation during the dark times.

Figure 4. The inset shows schematically the time dependence of the excitation light; this light is periodically blocked for a dark time, T_{off} , after each spectral collection time, T_{on} (170 ms). a, The autocorrelation function $C(n)$, for a single molecule under continuous 594-nm excitation ($T_{\text{off}} = 0$), n being the index number of the spectra. The dashed line is a double exponential fit, $C(n) = \{2,000 \exp(-0.35n) + 1,050 \exp(-0.03n)\} \text{ cm}^{-2}$. b, The $C(n)$ for the same molecule taken with a dark time $T_{\text{off}} = 0.5$ s and the same excitation rate during T_{on} . The fast component disappears, proving the spontaneous (thermal) fluctuation during the dark time. The dashed line is a single exponential fit with a decay constant $\gamma = 0.04$.



[\[Help with image viewing\]](#)

[\[Email Jumpstart To Image\]](#)

A room temperature, spontaneous fluctuations on the subpicosecond timescale are responsible for the broad spectral widths [Figure 1\(a\)](#). However, the spontaneous fluctuation we observed on the rather long timescale (hundreds of milliseconds) would be extremely difficult, if not impossible, to detect at room temperature in ensemble-averaged experiments. Although spontaneous fluctuations [\[12,13\]](#) have been studied for single molecules at cryogenic temperatures, the room-temperature fluctuations we observed have significantly larger magnitude and involve a thermally activated mechanism (rather than tunnelling).

The quasi-linear dependence of k_2 on excitation rate [Figure 3\(b\)](#), [Figure 3\(c\)](#) clearly indicates the photoinduced nature of the spectral fluctuations at the longer timescale. Although we cannot rule out the possibility of a quadratic dependence on excitation power, multiphoton processes (such as excited state absorption) are not likely to occur at the low power level ($<10^3$ W cm sup -2) used.

There are two possible mechanisms for the photoinduced spectral fluctuation. First, a molecule can access other ground-state potential minima with different spectra through relaxations from its singlet excited state, a phenomenon known as 'nonphotochemical hole burning' [\[14\]](#). Single-molecule 'nonphotochemical hole burning' has been observed at cryogenic temperature [\[15-17\]](#), but the spectral shifts are much smaller than those observed in our experiment. Second, the spectral fluctuations can also be associated with radiationless relaxations, probably from the triplet state. The energy released in each relaxation event is quickly dissipated into the substrate, and the original temperature of the system is re-established before the next photoexcitation. However, the energy released can lead to variations of the nuclear coordinates, resulting in a new spectrum in subsequent photoexcitations. At present, we are not able to distinguish experimentally between these two mechanisms. The slow rate of photoinduced fluctuation is associated with the small quantum efficiency for either of the two mechanisms. The apparently steeper slope in [Figure 3\(b\)](#) is probably associated with the higher photon energy of the 532-nm excitation.

For either the fast or slow spectral fluctuation component, both thermal and photoinduced contributions are possible. Dominated by the thermal fluctuation, k_1 receives little contribution, if any, from the photoinduced fluctuation because of its small quantum efficiency. Conversely, k_2 has some contribution from the thermal rate ($k_{2\text{ther}}$), but is often dominated by the photoinduced rate ($k_{2\text{pho}} = k_2 - k_{2\text{ther}}$) for a broad range of excitation intensity. Although it is difficult to extrapolate the slower $k_{2\text{ther}}$ at zero excitation rate [Figure 3\(b\)](#), [Figure 3\(c\)](#), $k_{2\text{ther}}$ can be determined by using the scheme shown in [Figure 4](#) inset and by evaluating the autocorrelation functions, $C(n)$, at different dark times, T_{off} . When neglecting the fast component k_1 , [Equation 2](#) where $\text{gamma} = k_{2\text{ther}} T_{\text{off}} + (k_{2\text{ther}} +$

$k_{2\text{pho}}T_{\text{on}}$ is a single exponential rate constant. Therefore, a longer dark time results in a faster decay of $C(n)$, as is evident by comparing the decay of the curve in Figure 4(b) to the slow component of the curve in Figure 4(a). In Figure 5(a), we plot γ as a function of T_{off} for several trajectories of a few molecules at a constant excitation rate during T_{on} . The slope of the fitted line gives $k_{2\text{ther}} = 0.02 \pm 0.01 \text{ s}^{-1}$, whereas the intercept results in $k_{2\text{pho}} = 0.02 \pm 0.01 \text{ s}^{-1}$.

$$\begin{aligned} C(n) &= C(0) \exp\{-nk_{2\text{ther}}(T_{\text{off}} + T_{\text{on}}) - nk_{2\text{pho}}T_{\text{on}}\} \\ &= C(0) \exp(-n\gamma) \end{aligned} \quad \text{Equation 2}$$

[\[Help with image viewing\]](#)

[\[Email Jumpstart To Image\]](#)

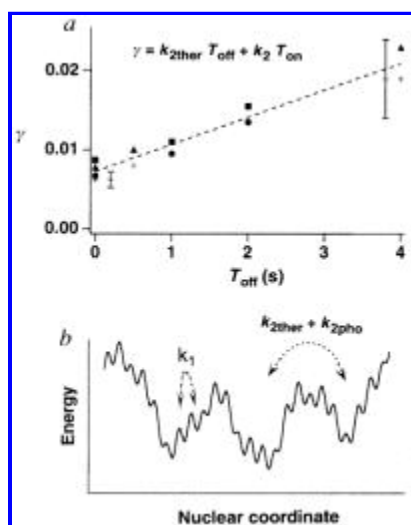


Figure 5. a, Plot of γ , the decay constant of $C(n)$, as a function of the dark time T_{off} . Data points derived from spectral trajectories of the same sulphorhodamine 101 molecule are labelled with the same symbols. The slope of the dashed line gives the slow thermal rate $k_{2\text{ther}} = 0.02 \pm 0.01 \text{ s}^{-1}$, while the intercept gives the photoinduced rate, $k_{2\text{pho}} = 0.02 \pm 0.01 \text{ s}^{-1}$ at the excitation rate of $2 \times 10^5 \text{ s}^{-1}$ during T_{on} (170 ms). b, Schematic of the potential energy surface of the nuclear coordinates. Our analyses of the spectral trajectories indicate the existence of two distinctly different types of barrier heights. The small barriers are associated with fast thermal fluctuation (k_1), and the large (gross) barriers are associated with the photoinduced ($k_{2\text{pho}}$) and slow thermal ($k_{2\text{ther}}$) fluctuations.

[\[Help with image viewing\]](#)

[\[Email Jumpstart To Image\]](#)

The large k_1 and the small $k_{2\text{ther}}$ indicate that there are two distinctly different types of barrier in the potential-energy surface of the nuclear coordinates. As illustrated schematically in a one-dimensional cross-section of the ground-state potential energy surface Figure 5(b), the local potential minima connected with the small barriers can be accessed through the fast thermal fluctuation (k_1), whereas the gross potential minima connected with the large barriers can only be accessed through the slow photoinduced fluctuation ($k_{2\text{pho}}$) and the much slower thermal fluctuation ($k_{2\text{ther}}$). Within each gross minimum, there is a spectral mean distribution (with variance of $\sigma_{a_1}^2$) associated with the different local minima. Independently, there is another spectral mean distribution (with variance of $\sigma_{a_2}^2$) associated with the different gross minima. The activation energies for k_1 and $k_{2\text{ther}}$ might be evaluated from the temperature dependence of the spectral trajectories.

Although a microscopic description of the nuclear coordinates awaits further studies, our room-temperature experiments have provided new insights into the general features of the potential-energy surface and the dynamical

properties of a single molecule in a particular environment. Similar structures of potential energy surfaces have been put forward for proteins [18], and the kind of analysis described here may allow them to be explored.

ACKNOWLEDGEMENTS. We thank R. Dunn, J. Trautman, P. Barbara, K. Eisenhal, C. Johnson, S. Colson and G. Holtom for discussions. Pacific Northwest National Laboratory is operated for the US Department of Energy (DOE) by Battelle. This work was supported by the Office of Basic Energy Sciences, Chemical Science Division, US DOE.

CORRESPONDENCE should be addressed to X.S.X. (e-mail: xs_xie@pnl.gov).

Received 22 May; accepted 18 November 1996.

REFERENCES

1. Betzig, E. & Chichester, R. J. *Science* 262, 1422-1425 (1993). [\[Context Link\]](#)
2. Nie, S. Chiu, D. T. & Zare, R. N. *Science* 266, 1018-1021 (1994). [\[Context Link\]](#)
3. Macklin, J. J., Trautman, J. K., Harris, T. D. & Brus, L. E. *Science* 272, 255-258 (1996). [Ovid Full Text](#) | [\[Context Link\]](#)
4. Trautman, J. K., Macklin, J. J., Brus, L. E. & Betzig, E. *Nature* 369, 40-42 (1994). [\[Context Link\]](#)
5. Xie, X. S., Bian, R. X. & Dunn, R. C. in *Focus of Multidimensional Microscopy Vol. 1* (eds Chen, P. C., Hwang, P. P., Wu, J. L., Wang, G. & Kim, H.) (World Scientific, Teaneck, NJ, in the press). [\[Context Link\]](#)
6. Xie, X. S. & Dunn, R. C. *Science* 265, 361-364 (1994). [\[Context Link\]](#)
7. Ambrose, W. P., Goodwin, P. M., Martin, J. C. & Keller, R. A. *Science* 265, 364-367 (1994). [\[Context Link\]](#)
8. Bian, R. X., Dunn, R. C., Xie, X. S. & Leung, P. T. *Phys. Rev. Lett.* 75, 4772-4775 (1995). [\[Context Link\]](#)
9. Schmidt, Th., Schutz, G. J., Baumgartner, W., Gruber, H. J. & Schindler, H. J. *Phys. Chem.* 99, 17662-17668 (1995). [\[Context Link\]](#)
10. Bernard, J., Fleury, L., Talon, H. & Orrit, M. *J. Chem. Phys.* 98, 850-859 (1993). [\[Context Link\]](#)
11. Basche, Th., Kummer, S. & Brauchle, C. *Nature* 373, 132-134 (1995). [\[Context Link\]](#)
12. Ambrose, P. A. & Moerner, W. E. *Nature* 349, 225-227 (1991). [\[Context Link\]](#)
13. Reilly, P. D. & Skinner, J. L. *J. Chem. Phys.* 102, 1540-1552 (1995). [\[Context Link\]](#)
14. Jankowlak, R. & Small, G. J. *Science* 237, 618-625 (1987). [\[Context Link\]](#)
15. Orrit, M. & Bernard, J. *Phys. Rev. Lett.* 65, 2716-2719 (1990). [\[Context Link\]](#)
16. Moerner, W. E. et al. *J. Phys. Chem.* 98, 7382-7389 (1994). [\[Context Link\]](#)
17. Basche, Th., Ambrose, W. P. & Moerner, W. E. *J. Opt. Soc. Am. B* 9, 829-836 (1992). [\[Context Link\]](#)

18. Frauenfelder, H. & Wolynes, P. G. Phys. Today 47, 58-64 (1994). [\[Context Link\]](#)

Copyright (c) 2000-2007 [Ovid Technologies, Inc.](#)

Version: OvidSP_UI01.00.02, SourceID 34391